

Article

# Wigner Function Non-Classicality Induced in a Charge Qubit Interacting with a Dissipative Field Cavity

Abdel-Baset A. Mohamed <sup>1,2,\*</sup>, Eied M. Khalil <sup>3</sup> , Afrah Y. AL-Rezami <sup>1,4</sup>  and Hichem Eleuch <sup>5,6,7</sup>

<sup>1</sup> Department of Mathematics, College of Science and Humanities in Al-Aflaj, Prince Sattam bin Abdulaziz University, Al-Aflaj 11942, Saudi Arabia; a.mohamed@psau.edu.sa

<sup>2</sup> Department of Mathematics, Faculty of Science, Assiut University, Assiut 71515, Egypt

<sup>3</sup> Department of Mathematics, College of Science, Taif University, P.O. Box 11099, Taif 21944, Saudi Arabia; eiedkhalil@tu.edu.sa

<sup>4</sup> Department of Statistics and Information, College of Commerce and Economics, Sana'a University, Sana'a 15542, Yemen; a.alrezamee@psau.edu.sa

<sup>5</sup> Department of Applied Physics and Astronomy, University of Sharjah, Sharjah 27272, United Arab Emirates; hichem.eleuch@adu.ac.ae

<sup>6</sup> Department of Applied Sciences and Mathematics, College of Arts and Sciences, Abu Dhabi University, Abu Dhabi 59911, United Arab Emirates

<sup>7</sup> Institute for Quantum Science and Engineering, Texas A&M University, College Station, TX 77843, USA

\* Correspondence: abdelbastm@aun.edu.eg



**Citation:** Mohamed, A.-B.A.; Khalil, E.M.; AL-Rezami, A.Y.; Eleuch, H. Wigner Function Non-Classicality Induced in a Charge Qubit Interacting with a Dissipative Field Cavity. *Symmetry* **2021**, *13*, 802. <https://doi.org/10.3390/sym13050802>

Academic Editors: Pedro D. Sacramento, Nikola Paunkovic and Jan Awrejcewicz

Received: 20 March 2021

Accepted: 29 April 2021

Published: 4 May 2021

**Publisher's Note:** MDPI stays neutral with regard to jurisdictional claims in published maps and institutional affiliations.



**Copyright:** © 2021 by the authors. Licensee MDPI, Basel, Switzerland. This article is an open access article distributed under the terms and conditions of the Creative Commons Attribution (CC BY) license (<https://creativecommons.org/licenses/by/4.0/>).

**Abstract:** We explore a superconducting charge qubit interacting with a dissipative microwave cavity field. Wigner distribution and its non-classicality are investigated analytically under the effects of the qubit–cavity interaction, the qubit–cavity detuning, and the dissipation. As the microwave cavity field is initially in an even coherent state, we investigate the non-classicality of the Wigner distributions. Partially and maximally frozen entanglement are produced by the qubit–cavity interaction, depending on detuning and cavity dissipation. It is found that the amplitudes and frequency of the Wigner distribution can be controlled by the phase space parameters, the qubit–cavity interaction and the detuning, as well as by the dissipation. The cavity dissipation reduces the non-classicality; this process can be accelerated by the detuning.

**Keywords:** charge–qubit system; quasi-probability wigner function; entanglement

## 1. Introduction

The decoherence and dissipation issues taint the dynamics of every quantum system. These effects reduce, distort or destroy the quantum phenomena, [1,2] such as: quantum coherence, squeezing, and quantum correlation. Moreover, decoherence is the most significant characteristic of an open quantum system. This quantum effect destroys the nonclassical correlations. Decoherence affects the entangled states and transforms them to mixed states [3]. Decoherence usually occurs as the system's constituents interact with the environment [4,5]. The effects of decoherence and dissipations on the dynamical features have been investigated in various quantum systems [6–9]. The interaction between the quantum systems and the environment usually leads to a decoherence/dissipation process, which reduces the quantum phenomena [10].

The decoherence and the dissipation effects might lead to spontaneous symmetry breaking or phase transition phenomena [11–15], which may occur in several dissipative quantum systems [16–19]. These effects erase the quantum information resources. In general, the decoherence and the dissipation effects can be investigated by various types of master equation [20–24] which can be employed to analyze the quantum dynamics of the systems.

To characterize quantum states and present valuable quantum information about the system states, quasi-probability distributions were introduced [25]. Wigner distribu-

tion (WD) is the first quasi-probability distribution that was introduced to determine the quantum corrections [26]. WD is an important tool to explore the non-classicality via its negative values [27–32]. There is a link between the WD negativity and the entanglement [33–36]; however, the negativity of the Wigner distribution is not sufficient to guaranty the non-classicality [37]. The negativity of the generalized Wigner function was used as an entanglement witness for hybrid bipartite states [38]. The non-Gaussianity of the Wigner function could be detected by its representation in the phase space. Based on the link between the WD negativity and the entanglement entropy, the non-gaussian nature and entanglement of spontaneous parametric nondegenerate triple-photon generation were investigated [39,40]. Experimentally, the Wigner function of a single photon is used to demonstrate non-classicality properties specific to non-Gaussian states [41]. It is found that a negative value of the Wigner function is a sufficient condition for non-Gaussianity of two-photon states [42].

Superconducting (SC) qubits or two-level systems of Josephson junctions are promising candidates for realizing quantum computation [43–46]. Recently, researchers have achieved significant progress in conceiving the quantum regime in these systems. It was reported that these qubits can be strongly coupled to a single-microwave photon [47,48]. Superconducting circuits present several potential applications, such as: realizing Fock states [49], implementing quantum algorithms [50], encoding [51], and realizing entanglement [52].

The decoherence and the dissipation effects on the WD nonclassicality were investigated in [53,54]. These studies were limited [55–57]. The WD non-classicality was explored for a cavity QED containing a high optical nonlinear medium and a quantum well [55], for weak dissipation rates. In [56], the effect of intrinsic decoherence on the WD dynamics of a cavity interacting resonantly with two coupled qubits was investigated. Under the phase-cavity-damping effect, the WD nonclassicality of a cavity field interacting with a qubit with a specific value of applied magnetic flux (half of the applied flux quantum) was studied [57].

In this paper, we explore the Wigner distribution non-classicality for a microwave cavity field interacting with a superconducting charge qubit. The consider system is an open quantum system interacting with the environment through cavity dissipation (the system energy is not conserved). The method used in this paper can be used to investigate the dynamics of quantum information resources of the Wigner distribution or a quasi-probability distribution in other qubit-cavity systems.

The paper is organized as follows: In Section 2, we present the physical scheme for a qubit–cavity system with cavity-damping effect. The dynamics and properties of the WD will be investigated in Section 3. Finally, in Section 4, we conclude our results.

## 2. Dissipative Qubit-Cavity System

We consider a charged qubit system that is described by a Cooper-pair box, containing two identical Josephson junctions, and placed into a microwave cavity. The general Hamiltonian for this system is given by [48,58,59]

$$\hat{H} = \omega \hat{\psi}^\dagger \hat{\psi} + E_z \hat{\sigma}_z - E_J \hat{\sigma}_x \cos[\phi \hat{I} + \frac{\pi}{\Phi_0} (\eta \hat{\psi} + \eta^* \hat{\psi}^\dagger)]. \quad (1)$$

where  $\phi = \frac{\pi \Phi_c}{\Phi_0}$  and  $\omega$  represent the frequency cavity field that has the creation operators to which  $\hat{\psi}^\dagger$ , and  $E_z$  denote the qubit charging energy.  $E_J$  is the coupling-energy Josephson junctions.  $\Phi_c$  represents the applied classical magnetic field and  $\Phi_0$  is the applied flux quantum.  $\hat{\sigma}_z$  and  $\hat{\sigma}_x$  are the Pauli matrix operators, which are represented in the basis formed by the excited  $|e\rangle$  and ground  $|g\rangle$  states. The constant  $\eta$  has units of the magnetic flux and depends on the geometrical design of the SC cavity.

Here, the Cooper-pair box works as a qubit in the microwave region where (1) the Cooper-pair box is in the middle of the microwave cavity. (2) The microwave cavity field is

not too strong, such that all higher orders of  $\frac{\pi\eta}{\Phi_0}$  are neglected except the first order. (3) We use the following operators:

$$\hat{\Lambda}_x = \hat{\sigma}_x \cos \phi + \hat{\sigma}_y \sin \phi, \hat{\Lambda}_y = (\hat{\sigma}_x \sin \phi - \hat{\sigma}_y \cos \phi), \hat{\Lambda}_z = \hat{\sigma}_z. \quad (2)$$

Consequently, the Hamiltonian of Equation (2) can be written as

$$\hat{H} = \omega \hat{\psi}^\dagger \hat{\psi} + E_z \hat{\Lambda}_z - E_J \hat{\Lambda}_x + \frac{\pi E_J \eta}{\Phi_0} \hat{\Lambda}_y (\hat{\psi} + \hat{\psi}^\dagger). \quad (3)$$

The operators  $\hat{\Lambda}_k (k = x, y, z)$  satisfy the following properties

$$[\hat{\Lambda}_x, \hat{\Lambda}_y] = 2i \hat{\Lambda}_z, [\hat{\Lambda}_y, \hat{\Lambda}_z] = 2i \hat{\Lambda}_x, [\hat{\Lambda}_z, \hat{\Lambda}_x] = 2i \hat{\Lambda}_y. \quad (4)$$

If the charge qubit–cavity system is interacting with the surrounding environment, different types of decoherence and dissipation affect the qubit–cavity system. To study the effect of the cavity dissipation on the time-dependent density matrix of the system, we consider the master equation,

$$\frac{d\hat{\rho}(t)}{dt} = -i[\hat{H}, \hat{\rho}(t)] + \gamma([\hat{\psi}\hat{\rho}(t), \hat{\psi}^\dagger] + [\hat{\psi}, \hat{\rho}(t)\hat{\psi}^\dagger]), \quad (5)$$

where  $\gamma$  represent dissipation. To solve Equation (5), we used two canonical transformations. We transform the states  $|e\rangle$  and  $|g\rangle$  to the states  $|1\rangle$  and  $|0\rangle$ , respectively, [60] as:

$$|1\rangle = \cos \theta |e\rangle + \sin \theta |g\rangle, \quad |0\rangle = \cos \theta |g\rangle - \sin \theta |e\rangle, \quad (6)$$

where  $\theta = \frac{1}{2} \tan^{-1}(\frac{E_z}{E_J})$ . With the rotating operators  $\hat{\chi}_+ = |1\rangle\langle 0|$ ,  $\hat{\chi}_- = |0\rangle\langle 1|$ , and  $\hat{\chi}_z = |1\rangle\langle 1| - |0\rangle\langle 0|$ , which satisfy the following properties

$$[\hat{\chi}_+, \hat{\chi}_-] = \hat{\chi}_z, [\hat{\chi}_z, \hat{\chi}_\pm] = \pm 2\hat{\chi}_\pm. \quad (7)$$

By using the above transforms and the rotating wave approximation ( $\hat{H}$  and  $\hat{\rho}(t)$  changes to  $\hat{H}_\chi$  and  $\hat{R}(t)$ , respectively), Equation (5) is rewritten as master equation,

$$\frac{d\hat{R}(t)}{dt} = -i[\hat{H}_\chi, \hat{R}(t)] + \gamma([\hat{\psi}\hat{R}(t), \hat{\psi}^\dagger] + [\hat{\psi}, \hat{R}(t)\hat{\psi}^\dagger]), \quad (8)$$

with

$$\hat{H}_\chi = \omega \hat{\psi}^\dagger \hat{\psi} + \omega_0 \hat{\chi}_z - \lambda (\hat{\psi} \hat{\chi}_+ + \hat{\chi}_- \hat{\psi}^\dagger), \quad (9)$$

where  $\lambda = \frac{\pi E_J}{\Phi_0} \cos^2 \zeta$ .  $\omega_0 = \sqrt{E_z^2 + E_J^2}$  represents the qubit frequency, which shifts the atomic energy levels to  $\pm \frac{1}{2} \sqrt{E_z^2 + E_J^2}$ . The operators  $\hat{\sigma}'$ s in terms the rotating operators  $\hat{\chi}'$ s are given by

$$\begin{aligned} \hat{\sigma}_x &= \cos \phi (\hat{\chi}_x \cos 2\theta - \hat{\chi}_z \sin 2\theta) - \hat{\chi}_y \sin \phi, \\ \hat{\sigma}_y &= \sin \phi (\hat{\chi}_x \cos 2\theta - \hat{\chi}_z \sin 2\theta) + \hat{\chi}_y \cos \phi, \\ \hat{\sigma}_z &= \hat{\chi}_z \cos 2\theta + \hat{\chi}_x \sin 2\theta. \end{aligned} \quad (10)$$

After that, the second canonical transformation  $Z(t) = e^{i\hat{H}t} R(t) e^{-i\hat{H}t}$  (that changes  $\hat{R}(t)$  to  $Z(t)$ ) is used with the secular approximation and the dressed-states (DS) method [61,62] for the case of a high-Q cavity. In the DS method, the microwave cavity field operators are rewritten in terms of the eigenstates' complete set of the Hamiltonian  $\hat{H}_\chi$ , and the oscillatory terms will be neglected. The eigenstates and eigenvalue of Hamiltonian:  $\hat{H}_\chi$

are given by  $|\varphi_n^\pm\rangle = a_n^\pm|1, n\rangle \pm a_n^\mp|0, n+1\rangle$  ( $n = 0, 1, 2, \dots$ ), with  $a_n^\pm = \frac{1}{\sqrt{2}}\sqrt{1 \mp \frac{\delta}{\eta_n}}$ ,  $\eta_n = \sqrt{\delta^2 + \lambda^2(n+1)}$ . The dynamics of the density matrix  $Z(t)$  is given by

$$\dot{Z}(t) = e^{i\hat{H}t}\gamma([\psi\hat{R}(t), \hat{\psi}^\dagger] + [\hat{\psi}, \hat{R}(t)\hat{\psi}^\dagger])e^{-i\hat{H}t}. \quad (11)$$

The off-diagonal elements ( $m \neq n$ ) of the matrix  $Z(t)$  are given by

$$\begin{aligned} x_{mn} &= \langle \varphi_m^+ | z(t) | \varphi_n^+ \rangle = x_{mn}(0)e^{-\gamma(m+n+a_m^{-2}+a_n^{-2})t}, \\ y_{mn} &= \langle \varphi_m^- | z(t) | \varphi_n^- \rangle = y_{mn}(0)e^{-\gamma(m+n+a_m^{+2}+a_n^{+2})t}, \\ w_{mn} &= \langle \varphi_m^+ | z(t) | \varphi_n^- \rangle = w_{mn}(0)e^{-\gamma(m+n+a_m^{-2}+a_n^{+2})t}, \\ u_{mn} &= \langle \varphi_m^- | z(t) | \varphi_n^+ \rangle = u_{mn}(0)e^{-\gamma(m+n+a_m^{+2}+a_n^{-2})t}. \end{aligned} \quad (12)$$

while the diagonal elements of the  $Z(t)$  satisfy the differential equations

$$\dot{x}_n(t) = 2\gamma[f_{n+1}^{+2}x_{n+1}(t) + g_{n+1}^{+2}y_{n+1}(t) - (n + a_n^2)x_n(t)]. \quad (13)$$

$$\dot{y}_n(t) = 2\gamma[f_{n+1}^{-2}y_{n+1}(t) + g_{n+1}^{-2}x_{n+1}(t) - (n + a_n^{+2})y_n(t)]. \quad (14)$$

where  $f_n^\pm = \sqrt{n}a_{n-1}^\pm a_n^\pm + \sqrt{n+1}a_{n-1}^\mp a_n^\mp$ , and  $g_n^\pm = \sqrt{n}a_{n-1}^\pm a_n^\mp - \sqrt{n+1}a_{n-1}^\mp a_n^\pm$ . Here, we assumed that the SC-qubit initial density matrix is the density matrix  $|1\rangle\langle 1|$ , while the cavity is considered initially in an even, coherent state,

$$|\psi(0)\rangle_C = \frac{1}{\sqrt{A}}[|\alpha\rangle + |-\alpha\rangle] = \sum_{n=0}^{\infty} p_n |n\rangle, \quad (15)$$

with the photon distribution function  $p_n$ ,

$$p_n = \frac{[1 + (-1)^n]\alpha^n e^{-\frac{1}{2}|\alpha|^2}}{2(1 + \langle \alpha | -\alpha \rangle)\sqrt{n!}}. \quad (16)$$

Therefore, in the space states  $\{|1\rangle, |0\rangle\}$ , the density matrix  $R = [\sum_{mn} R_{ij}^{mn}]$ ,  $R_{ij}^{mn}$  are given by

$$R_{11} = \begin{cases} [a_m^+ a_n^+ e^{-i\pi_1^+ t} x_{mn} + a_m^- a_n^- e^{-i\pi_1^- t} y_{mn} + a_m^+ a_n^- e^{-i\pi_2^+ t} w_{mn} \\ \quad + a_m^- a_n^+ e^{-i\pi_2^- t} u_{mn}] |m\rangle\langle n|, & m \neq n; \\ [a_n^{+2} x_n + a_n^{-2} y_n + 2p_n^* p_n a_n^{+2} a_n^{+2} e^{-\gamma(2n+1)t} \cos(2\eta_n t)] |m\rangle\langle n|, & m = n. \end{cases} \quad (17)$$

$$R_{00} = \begin{cases} [a_m^- a_n^- e^{-i\pi_1^+ t} x_{mn} + a_m^+ a_n^+ e^{-i\pi_1^- t} y_{mn} - a_m^- a_n^+ e^{-i\pi_2^+ t} w_{mn} \\ \quad - a_m^+ a_n^- e^{-i\pi_2^- t} u_{mn}] |m\rangle\langle n|, & m \neq n; \\ [a_n^{-2} x_n + a_n^{+2} y_n - 2p_n^* p_n a_n^{+2} a_n^{+2} e^{-\gamma(2n+1)t} \cos(2\eta_n t)] |m\rangle\langle n|, & m = n; \\ [\gamma \int_0^t [x_0 + y_0] d\tau] |0\rangle\langle 0|, & m=n=0. \end{cases} \quad (18)$$

$$R_{10} = R_{01}^\dagger = [a_m^- a_n^+ e^{-i\pi_1^+ t} x_{mn} - a_m^+ a_n^- e^{-i\pi_1^- t} y_{mn} + a_m^- a_n^- e^{-i\pi_2^+ t} w_{mn} \\ - a_m^+ a_n^+ e^{-i\pi_2^- t} u_{mn}] |m\rangle\langle n|, \quad (19)$$

where  $\pi_1^\pm = \omega(m-n) \pm \eta_m \mp \eta_n$  and  $\pi_2^\pm = \omega(m-n) \pm \eta_m - \pm \eta_n$ . By using the inverse of the considered canonical transformations, the time-dependent qubit-cavity system is given by

$$\begin{aligned} \rho(t) = & \sum_{m,n} [R_{11} \cos^2 \theta + R_{00} \sin^2 \theta - \frac{1}{2}(R_{10} + R_{01}) \sin 2\theta] |m, e\rangle \langle n, e| \\ & + [R_{00} \cos^2 \theta + R_{11} \sin^2 \theta - \frac{1}{2}(R_{10} + R_{01}) \sin 2\theta] |m, g\rangle \langle n, g| \\ & + [R_{10} \cos^2 \theta - R_{01} \sin^2 \theta + \frac{1}{2}(R_{11} - R_{00}) \sin 2\theta] |m, e\rangle \langle n, g| \\ & + [R_{01} \cos^2 \theta - R_{10} \sin^2 \theta + \frac{1}{2}(R_{11} - R_{00}) \sin 2\theta] |m, g\rangle \langle n, e|. \end{aligned} \quad (20)$$

### 3. Wigner Distribution (WD)

The phase space Wigner distribution for the quantum state  $\hat{\rho}(t)$  is defined by [25,63,64]:

$$W(p, q) = \frac{2}{\pi} \sum_{n=0}^{\infty} (-1)^n \langle \mu, n | \hat{\rho}(t) | \mu, n \rangle, \quad (21)$$

$\mu = p + iq$  is the parameter of the intensity of the coherent field  $|\mu, n\rangle = e^{p(\hat{\psi}^+ - \hat{\psi}) + iq(\hat{\psi}^+ + \hat{\psi})} |n\rangle$ . WD is a good indicator of the phase space information and non-classicality of a quantum state, based on its density matrix. For the reduced density matrix of the cavity field,  $\rho^f = \sum_{mn} \rho_{mn}^f$ , the WD is given by [25,63,64]

$$\begin{aligned} W(p + iq) = & \frac{2}{\pi} \sum_{k=0}^{\infty} (-1)^k \sum_{m,n=0}^{\infty} \frac{k! |p + iq|^{-2k} e^{-(p^2 + q^2)}}{\sqrt{m!n!}} (p + iq)^{*m} (p + iq)^n \\ & \times L_m^{m-k}(p^2 + q^2) \rho_{mn}^f L_n^{n-k}(p^2 + q^2), \end{aligned} \quad (22)$$

$L_n^{m-n}(p^2 + q^2)$  is the associated Laguerre formula. The WD positivity is an indicator of the classicality and the minimization uncertainty, while the WD negativity indicates the non-classicality [56,57]. In Figures 1–6, the WD  $W(p + iq)$  and its partial distributions (as:  $W(p)$ ,  $W(q)$  and  $W(t)$ ) are plotted to display the effects of the qubit-cavity interaction and the dissipation in the resonance and off-resonance cases. Figure 1a, displays the behavior of  $W(p + iq)$  when the microwave field cavity is initially in an even coherent state,  $\frac{1}{\sqrt{2}}[|\alpha\rangle + |-\alpha\rangle]$ , in the phase space:  $p \in [-2\pi, 2\pi]$  and  $q \in [0, \pi]$ . The WD has symmetrical interference peaks and bottoms around the two original peaks, which their heights and depths represent the positive and negative values of the WD. The interference peaks and bottoms in the behavior of the WD is due to the superposition of the even coherent state. The classicality of the positive parts, and the non-classicality of the negative parts of the WD are clearly distinguishable and are a natural signature of the properties of the initial, even coherent state.

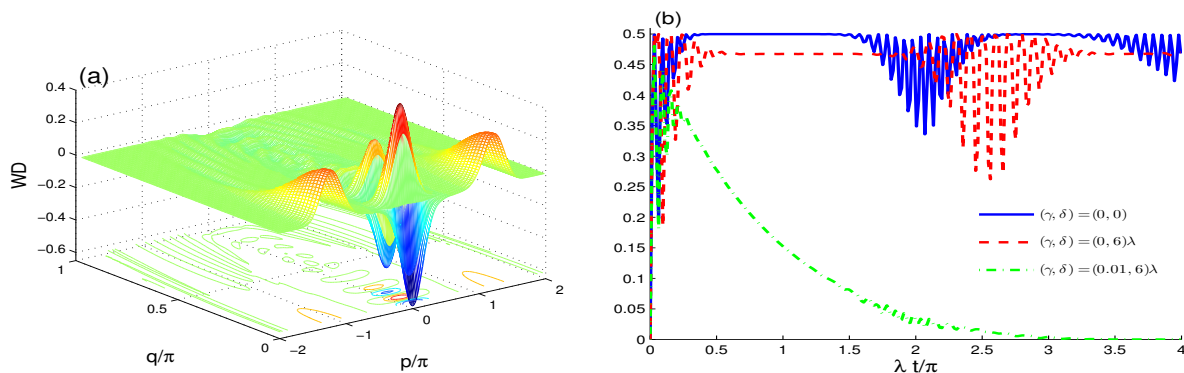


**Figure 1.** The Wigner distribution of the initial even coherent state with  $\alpha = 4$  in (a). In (b) the negativity entanglement  $N(t)$  for  $\alpha = 4$  and different cases:  $(\gamma, \delta) = (0, 0)$ ,  $(\gamma, \delta) = (0, 6)\lambda$  and  $(\gamma, \delta) = (0.01, 0)$ .

To investigate the time evolution of the WD, we illustrate it at different times. Based on the negativity entanglement between the SC-qubit and the coherent cavity field, the WD will be shown at the times of a partial and maximal qubit-cavity entanglement. The simplest definition of the negativity entanglement  $N(t)$  is the sum of negative eigenvalues of the partial transposition matrix for the qubit-cavity density matrix [65]. The qubit-cavity system has a maximally entangled state when  $N(t) = 0.5$ , and is in a disentangled state for  $N(t) = 0$ . Otherwise, the system has a partial entanglement. Figure 1b, shows the dynamics of the negativity entanglement  $N(t)$  under the effect of the unitary qubit-cavity interaction (solid curve), the detuning (dashed curve) and the dissipation (dash-dot curve). By starting the qubit-cavity interaction, the negativity grows and oscillates to show the generated partial and maximal entanglement between the charge-qubit and the coherent cavity field. In some time intervals, the negativity stabilizes into maximal entanglement, i.e., the qubit-cavity entanglement, which may be frozen in these intervals (referring to the phenomenon of frozen maximal entanglement). The dashed curve shows that the non-zero detuning leads to the reduction in the amplitudes and minima of the negativity as well as to the increase in the frozen negativity entanglement time windows. Dash-dot curve illustrates the effect of the dissipation that deteriorates the generated qubit-cavity entanglement, which completely vanishes after a particular time. The charge-qubit and the coherent cavity field are then in a disentangled state.

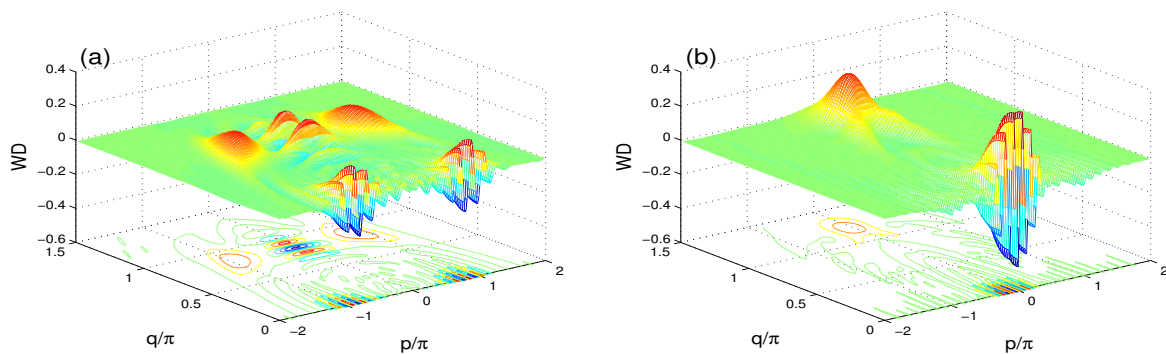


**Figure 2.** The WD at  $\lambda t = \pi$  in (a) and at  $\lambda t = 2.069\pi$  in (b) for  $\alpha = 4$ ,  $\gamma = 0$  and the resonance case  $\delta = 0$ .

In Figure 2, the Wigner distribution  $W(p + iq)$  is shown in the region  $p \in [0, 2\pi]$  and  $q \in [0, 1.5\pi]$  for two different normalized times,  $\lambda t = \pi$  in (a), at which the qubit-cavity state is in a maximally entangled state, and  $\lambda t = 2.069\pi$  in (b), which corresponds to a partial entanglement. We note that the qubit-cavity interaction leads to notable changes in the distribution of the positive and the negative regions of the WD. The distribution amplitudes of the symmetrical interference peaks and bottoms depend on the considered time  $\lambda t$ . For the case  $\lambda t = \pi$ , the main interference peaks and bottoms are around  $p = \pm\pi$ . While for the case  $\lambda t = 2.069\pi$ , the centers of the main interference peaks and bottoms are at the axis  $p = 0$ .

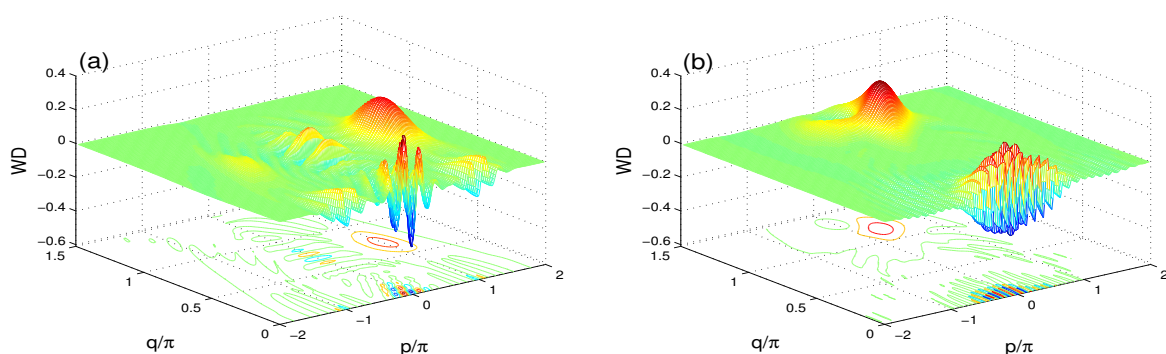


**Figure 3.** The WD at the scaled times  $\lambda t = \pi$  in (a) and at  $\lambda t = 2.069\pi$  in (b) for  $\alpha = 4$ ,  $\gamma = 0$  and the off-resonant case  $\delta = 6\lambda$ .

Figure 3, exhibits the effect of the detuning between the SC-qubit and the coherent cavity field on the WD  $W(p + iq)$  for  $\delta = 6\lambda$ . For this off-resonance case, the symmetric distribution of the interference peaks and bottoms disappears. The dependence of the peak and bottom distribution (their amplitudes, places, interference and frequency) and on the phase space parameters  $p$  and  $q$  is affected by the detuning. By comparing the resonance and off-resonance cases, we find that the increase in the detuning leads to the reduction in the amplitudes, interference and frequency of the peaks as well as the bottoms of the Wigner distribution.

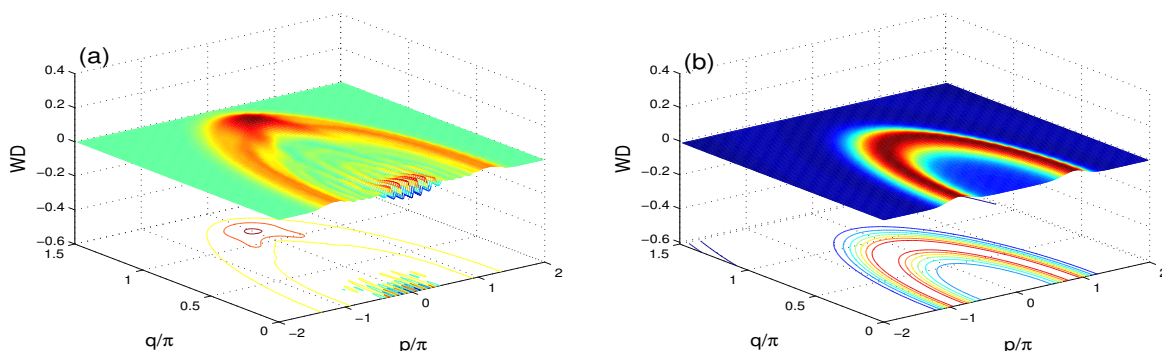


Figure 4. The WD is plotted at  $\lambda t = 2.069\pi$  for  $\alpha = 4, \delta = 0$  and the different values  $\gamma = 0.01$  in (a) and  $\gamma = 0.05$  in (b).

The effect of the coupling of the surrounding environment is shown in Figure 4 for the same parameter set of Figure 2b, but with non-zero damping values  $\gamma$ . We note that the increase in the dissipation leads to the reduction in the heights and depths of the peaks and bottoms of the symmetric WD. For large value of the dissipation  $\gamma = 0.05$ , the classicality (positive parts) and the non-classicality (negative parts) of the WD are approximately disappeared. We can deduce that the dissipation reduces the positive and the negative regions of the Wigner distribution.

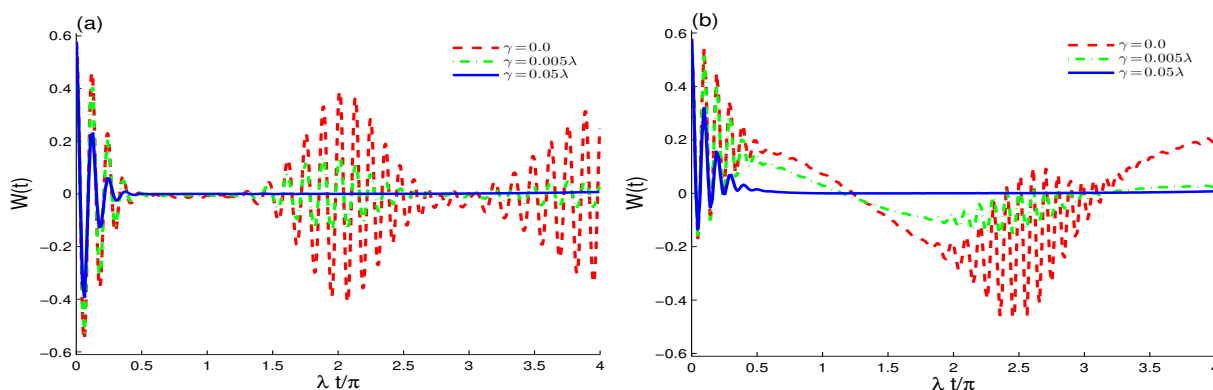
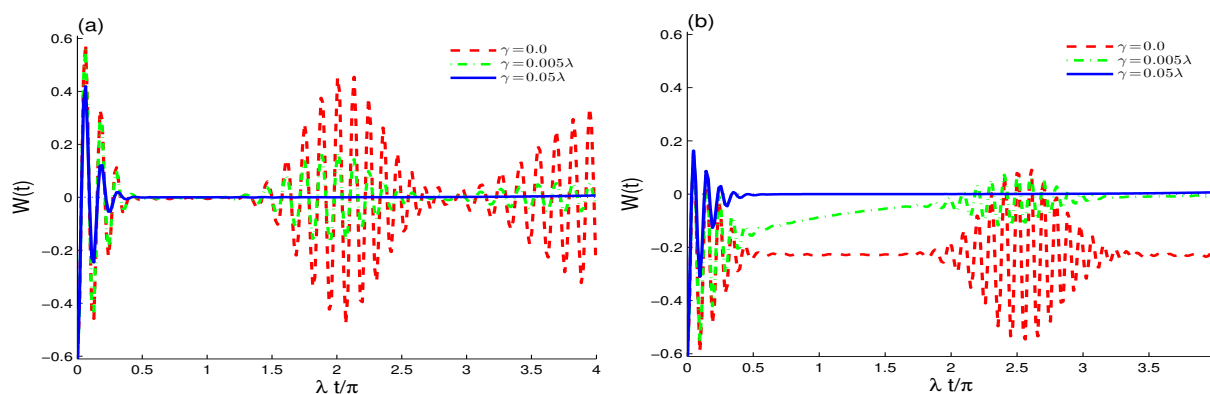


Figure 5. WD at the fixed value  $\mu_{max} = 0.009296\pi - 0.06127\pi i$  for  $\alpha = 4$  and the different values  $\gamma = 0.0, 0.005\lambda, 0.05\lambda$  with  $\delta = 0$  in (a) and  $\delta = 6\lambda$  in (b).

Figures 5 and 6 illustrates the effects of the dissipation and the qubit-field detuning on the dynamics of the non-classicality of the  $W(t)$  for the fixed point in the  $(p, q)$ -phase space,  $\mu_{max} = (p, q) = (0.009296\pi, -0.06127\pi)$ , which corresponds to the largest positive value of the initial WD (see Figure 1a). For the resonance case  $\delta = 0$  without the dissipation effect  $\gamma = 0.0$ , the Wigner distribution oscillates between its positive and negative values, showing that the qubit-cavity interaction generates classicality and non-classicality information. The Wigner distribution oscillates. It also illustrates collapses and revival phenomena. In the collapse intervals ( $W(t) = 0$ ), the WD has no classical or quantum information. By comparing the results of the negativity entanglement  $N(t)$  and the time evolution of the negativity of  $W(t)$ , we observe that they have similar dynamical behavior, where:

(1) The frozen maximal entanglement intervals  $N(t) = 0.5$  corresponds to the collapse intervals of the WD  $W(t) = 0$ . (2) The minima of the oscillatory behaviors of the  $N(t)$  and  $W(t)$  occur at the same times. The relationship between the negativity entanglement and the negativity of the WD confirms that the WD can be an indicator of the entanglement. Dashed and dash-dot curves show the effect of the dissipation on the dynamics of the WD  $W(t)$ . The amplitudes of the oscillations are reduced by the enhancement of the dissipation; therefore, the classical and quantum information of the Wigner distribution is completely erased.



**Figure 6.** WD at the fixed value  $\mu_{min} = 0.009296\pi - 0.06127\pi i$  for  $\alpha = 4$  and the different values  $\gamma = 0.0, 0.005\lambda, 0.05\lambda$  with  $\delta = 0$  in (a) and  $\delta = 6\lambda$  in (b).

In Figure 5b, the dynamics of the largest positive value of the WD is shown for the off-resonance case  $\delta = 6\lambda$ . We note that the detuning between the charge–qubit and the coherent cavity field enhances the oscillation frequency and the non-classicality of the WD. We also observe collapse intervals of the WD ( $W(t) = 0$ ). In addition, the detuning accelerates the effect of the dissipation, i.e., it accelerates the erasing of the classical and quantum information of the WD. The non-classicality dynamics of the  $W(t)$  for the fixed point in the phase space  $\mu_{min} = 0$ , which corresponds to the largest negative-value for the initial WD is displayed in Figure 6a. For the resonance case  $\delta = 0$ , we have the same behavior as the previous case of Figure 5a. While for the off-resonance case  $\delta = 6\lambda$ , we observe that the detuning leads to a downshift in the average of the Wigner distribution, from  $W(t) = 0$  to  $W(t) = -0.2$ . This means that the detuning increases the non-classicality of the Wigner distribution, and accelerates the erasing of its classical and quantum information due to the dissipation.

#### 4. Conclusions

In this contribution, we have analytically analyzed the entanglement and the non-classicality for a superconducting Cooper-pair box that contains two identical Josephson junctions, interacting with an open microwave cavity field. Our investigation is based on the effects of the qubit–cavity interaction, the resonance/off-resonance case and the coupling to the external environment. When the microwave cavity field is initially in an even coherent state, the link between the negativity entanglement and the non-classicality of the Wigner function is investigated. Without the dissipation effect, the negativity oscillates and presents frozen maximal entanglement phenomenon, which are affected by the detuning and reduced by the dissipation. The dependence of the amplitudes, interference and frequency of the Wigner distribution on the phase space parameters present notable changes due to the qubit–cavity interaction, the detuning and the cavity damping. The amplitudes, interference and frequency of the Wigner distribution crucially depend on the increase in the detuning. The detuning reshapes the non-classicality dynamics. Furthermore, it speeds up the erasure of the classical and quantum correlation of the Wigner distribution.

**Author Contributions:** Conceptualization, A.-B.A.M.; Data curation, A.Y.A.-R.; Investigation, A.-B.A.M.; Methodology, E.M.K.; Supervision, H.E.; Visualization, H.E. and A.Y.A.-R.; Writing original draft, A.-B.A.M. and E.M.K.; Writing review and editing, H.E. All authors have read and agreed to the published version of the manuscript.

**Funding:** Not applicable.

**Institutional Review Board Statement:** Not applicable.

**Informed Consent Statement:** Not applicable.

**Data Availability Statement:** Not applicable.

**Acknowledgments:** Taif University Researchers Supporting Project number (TURSP-2020/17), Taif University, Taif, Saudi Arabia.

**Conflicts of Interest:** The authors declare no conflict of interest.

## References

- Roman, S.; Kossakowski, A.; Ohya, M. *Information Dynamics and Open Systems: Classical and Quantum Approach*; Springer: New York, NY, USA, 1997.
- Attal, S.; Joye, A.; Alain, P. *Open Quantum Systems II: The Markovian Approach*; Springer: Berlin/Heidelberg, Germany, 2006.
- Pikovski, I.; Zych, M.; Costa, F.; Brukner, C. Time dilation in quantum systems and decoherence. *New J. Phys.* **2017**, *19*, 025011. [[CrossRef](#)]
- Eric R.B.; Peter J.R. Quantum decoherence in mixed quantum-classical systems: Nonadiabatic processes. *J. Chem. Phys.* **1995**, *103*, 8130.
- Eleuch, H.; Rotter, I. Clustering of exceptional points and dynamical phase transitions. *Phys. Rev. A* **2016**, *93*, 042116. [[CrossRef](#)]
- Mohamed, A.-B.A.; Eleuch, H.; Ooi, C.H.R. Quantum coherence and entanglement partitions for two driven quantum dots inside a coherent micro cavity. *Phys. Lett. A* **2019**, *383*, 125905. [[CrossRef](#)]
- Mohamed, A.-B.A.; Hessian, H.A.; Eleuch, H. Robust correlations in a dissipative two-qubit system interacting with two coupled fields in a non-degenerate parametric amplifier. *Quantum Inf. Process.* **2019**, *18*, 327. [[CrossRef](#)]
- Mohamed, A.-B.A.; Eleuch, H.; Ooi, C.H.R. Non-locality Correlation in Two Driven Qubits Inside an Open Coherent Cavity: Trace Norm Distance and Maximum Bell Function. *Sci. Rep.* **2019**, *9*, 19632. [[CrossRef](#)] [[PubMed](#)]
- Sete, A.E.; Eleuch, H. High-efficiency quantum state transfer and quantum memory using a mechanical oscillator. *Phys. Rev. A* **2015**, *91*, 032309. [[CrossRef](#)]
- Ikram, M.; Li, F.L.; Zubairy, M.S. Disentanglement in a two-qubit system subjected to dissipation environments. *Phys. Rev. A* **2007**, *75*, 062336. [[CrossRef](#)]
- Brauner, T. Spontaneous Symmetry Breaking and Nambu-Goldstone Bosons in Quantum Many-Body Systems. *Symmetry* **2010**, *2*, 609. [[CrossRef](#)]
- Arraut, I. The Quantum Yang-Baxter Conditions: The Fundamental Relations behind the Nambu-Goldstone Theorem. *Symmetry* **2019**, *11*, 803. [[CrossRef](#)]
- Nambu, Y. Spontaneous Breaking of Lie and Current Algebras. *J. Stat. Phys.* **2004**, *115*, 7. [[CrossRef](#)]
- Nambu, Y. From Yukawa's Pion to Spontaneous Symmetry Breaking. *J. Phys. Soc. Jpn.* **2007**, *76*, 111002. [[CrossRef](#)]
- Nambu, Y.; Jona-Lasrniot, G. Dynamical Model of Elementary Particles Based on an Analogy with Superconductivity. II. *Phys. Rev.* **1961**, *124*, 246. [[CrossRef](#)]
- Wilmington, H.; Kastoryano, M.J.; Werner, A.H.; Eisert, J. Emergence of spontaneous symmetry breaking in dissipative lattice systems. *J. Math. Phys.* **2017**, *58*, 033302. [[CrossRef](#)]
- Hannukainen, J.; Larson, J. Dissipation-driven quantum phase transitions and symmetry breaking. *Phys. Rev. A* **2018**, *98*, 042113. [[CrossRef](#)]
- Booker, C.; Buča, B.; Jaksch, D. Non-stationarity and dissipative time crystals: Spectral properties and finite-size effects. *New J. Phys.* **2020**, *22*, 085007. [[CrossRef](#)]
- Garbe, L.; Wade, P.; Minganti, F.; Shammah, N.; Felicetti, S.; Nori, F. Dissipation-induced bistability in the two-photon Dicke model. *Sci. Rep.* **2020**, *10*, 13408. [[CrossRef](#)] [[PubMed](#)]
- Lindblad, G. On the generators of quantum dynamical semigroups. *Commun. Math. Phys.* **1976**, *119*, 48. [[CrossRef](#)]
- Gorini, V.; Kossakowski, A.; Sudarsahan, E.C. Completely positive semigroups of n-level systems. *J. Math. Phys.* **1976**, *17*, 821. [[CrossRef](#)]
- Redfield, A. The theory of relaxation processes. In *Advances in Magnetic Resonance, Advances in Magnetic and Optical Resonance*; Waugh, J.S., Ed.; Academic Press: Cambridge, MA, USA, 1965; Volume 1.
- Puri, R.R. *Mathematical Methods of Quantum Optics*; Springer: Berlin, Germany, 2001.
- Milburn, G.J. Intrinsic decoherence in quantum mechanics. *Phys. Rev. A* **1991**, *44*, 5401. [[CrossRef](#)]
- Cahill, K.E.; Glauber, R.J. Density Operators and Quasiprobability Distributions. *Phys. Rev.* **1969**, *117*, 1882. [[CrossRef](#)]
- Wigner, E.P. On the Quantum Correction For Thermodynamic Equilibrium. *Phys. Rev.* **1932**, *47*, 749. [[CrossRef](#)]

27. Hillery, M.; O'Connell, R.F.; Scully, M.O.; Wigner, E.P. Distribution functions in physics: Fundamentals. *Phys. Rep.* **1984**, *106*, 121. [[CrossRef](#)]
28. Mohamed, A.-B.; Eleuch, H. Quasi-probability information in a coupled two-qubit system interacting non-linearly with a coherent cavity under intrinsic decoherence. *Sci. Rep.* **2020**, *10*, 13240. [[CrossRef](#)] [[PubMed](#)]
29. Ghorbani, M.; Faghihi, M.J.; Safari, H. Wigner function and entanglement dynamics of a two-atom two-mode nonlinear Jaynes-Cummings model. *J. Opt. Soc. Am. B* **2017**, *34*, 1884. [[CrossRef](#)]
30. Ren, G.; Zhang, W. Nonclassicality of superposition of photon-added two-mode coherent states. *Optik* **2019**, *181*, 191. [[CrossRef](#)]
31. Harder, G.; Silberhorn, C.; Rehacek, J.; Hradil, Z.; Motka, L.; Stoklasa, B.; Sánchez-Soto, L.L. Local sampling of the Wigner function at telecom wavelength with loss-tolerant detection of photon statistics. *Phys. Rev. Lett.* **2016**, *116*, 133601. [[CrossRef](#)]
32. Weiher, K.; Agudelo, E.; Bohmann, M. Conditional nonclassical field generation in cavity QED. *Phys. Rev. A* **2019**, *100*, 043812. [[CrossRef](#)]
33. Peres, A. Separability Criterion for Density Matrices. *Phys. Rev. Lett.* **1996**, *77*, 1413. [[CrossRef](#)]
34. Horodecki, P. Separability criterion and inseparable mixed states with positive partial transposition. *Phys. Lett. A* **1997**, *232*, 333. [[CrossRef](#)]
35. Horodecki, M.; Horodecki, P.; Horodecki, R. Separability of mixed states: Necessary and sufficient conditions. *Phys. Lett. A* **1996**, *223*, 1–8. [[CrossRef](#)]
36. Wootters, W.K. Entanglement of Formation of an Arbitrary State of Two Qubits. *Phys. Rev. Lett.* **1998**, *80*, 2245. [[CrossRef](#)]
37. Banerji, A.; Singh, R.P.; Bandyopadhyay, A. Entanglement measure using Wigner function: Case of generalized vortex state formed by multiphoton subtraction. *Optics Commun.* **2014**, *330*, 85–90. [[CrossRef](#)]
38. Arkhipov, I.I.; Barasiński, A.; Svozilík, J. Negativity volume of the generalized Wigner function as an entanglement witness for hybrid bipartite states. *Sci. Rep.* **2018**, *8*, 16955. [[CrossRef](#)]
39. Albarelli, F.; Genoni, M.G.; Paris, M.G.A. Resource theory of quantum non-Gaussianity and Wigner negativity. *Phys. Rev. A* **2018**, *98*, 052350. [[CrossRef](#)]
40. Zhang, D.; Cai, Y.; Zheng, Z.; Barral, D.; Zhang, Y.g.; Xiao, M.; Bencheikh, K. Non-Gaussian nature and entanglement of spontaneous parametric nondegenerate triple-photon generation. *Phys. Rev. A* **2021**, *103*, 013704. [[CrossRef](#)]
41. Walschaers, M.; Fabre, C.; Parigi, V.; Treps, N. Entanglement and Wigner Function Negativity of Multimode Non-Gaussian States. *PRL* **2017**, *119*, 183601. [[CrossRef](#)]
42. Douce, T.; Eckstein, A.; Walborn, S.P.; Khoury, A.Z.; Ducci, S.; Keller, A.; Coudreau, T.; Milman, P. Direct measurement of the biphoton Wigner function through two-photon interference. *Sci. Rep.* **2013**, *3*, 3530. [[CrossRef](#)]
43. You, J.Q.; Nori, F. Superconducting Circuits and Quantum Information. *Phys. Today* **2005**, *58*, 42. [[CrossRef](#)]
44. Clarke, J.; Wilhelm, F.K. Superconducting quantum bits. *Nature* **2008**, *453*, 1031. [[CrossRef](#)]
45. Obada, A.-S.F.; Hessian, H.A.; Mohamed, A.-B.A.; Homid, A.H. Efficient protocol of N-bit discrete quantum Fourier transform via transmon qubits coupled to a resonator. *Quantum Inf. Process.* **2014**, *13*, 475. [[CrossRef](#)]
46. Abovyan, G.A.; Kryuchkyan, Y.G. Quasienergies and dynamics of a superconducting qubit in a time-modulated field. *Phys. Rev. A* **2013**, *88*, 033811. [[CrossRef](#)]
47. Wallraff, A.; Schuster, D.I.; Blais, A.; Frunzio, L.; Huang, R.; Majer, J.; Kumar, S.; Girvin, S.M.; Schoelkopf, R.J. Strong coupling of a single photon to a superconducting qubit using circuit quantum electrodynamics. *Nature* **2004**, *431*, 162. [[CrossRef](#)] [[PubMed](#)]
48. Liu, Y.-X.; Wei, L.F.; Nori, F. Generation of nonclassical photon states using a superconducting qubit in a microcavity. *Europhys. Lett.* **2004**, *67*, 941. [[CrossRef](#)]
49. Hofheinz, M.; Weig, E.M.; Ansmann, M.; Bialczak, R.C.; Lucero, E.; Neeley, M.; O'Connell, A.D.; Wang, H.; Martinis, J.M.; Cleland, A.N. Generation of Fock states in a superconducting quantum circuit. *Nature* **2008**, *454*, 310. [[CrossRef](#)]
50. DiCarlo, L.; Chow, J.M.; Gambetta, J.M.; Bishop, L.S.; Johnson, B.; Schuster, D.I.; Majer, J.; Blais, A.; Frunzio, L.; Girvin, S.M.; et al. Demonstration of two-qubit algorithms with a superconducting quantum processor. *Nature* **2009**, *460*, 240. [[CrossRef](#)]
51. Vlastakis, B.; Kirchmair, G.; Leghtas, Z.; Nigg, S.E.; Frunzio, L.; Girvin, S.M.; Mirrahimi, M.; Devoret, M.H.; Schoelkopf, R.J. Deterministically Encoding Quantum Information Using 100-Photon Schrödinger Cat States. *Science* **2013**, *342*, 607. [[CrossRef](#)]
52. Riste, D.; Dukalski, M.; Watson, C.A.; de Lange, G.; Tiggelman, M.J.; Blanter, Y.M.; Lehnert, K.W.; Schouten, R.N.; DiCarlo, L. Deterministic entanglement of superconducting qubits by parity measurement and feedback. *Nature* **2013**, *502*, 350. [[CrossRef](#)]
53. Teh, R.Y.; Sun, F.-X.; Polkinghorne, R.E.S.; He, Q.Y.; Gong, Q.; Drummond, P.D.; Reid, M.D. Dynamics of transient cat states in degenerate parametric oscillation with and without nonlinear Kerr interactions. *Phys. Rev. A* **2020**, *101*, 043807. [[CrossRef](#)]
54. Meng, X.-G.; Goan, H.-S.; Wang, J.-S.; Zhang, R. Nonclassical thermal-state superpositions: Analytical evolution law and decoherence behavior. *Opt. Commun.* **2018**, *411*, 15. [[CrossRef](#)]
55. Mohamed, A.-B.; Eleuch, H. Non-classical effects in cavity QED containing a nonlinear optical medium and a quantum well: Entanglement and non-Gaussianity. *Eur. Phys. J. D* **2015**, *69*, 191.
56. Mohamed, A.-B.A.; Eleuch, H.; Obada, A.-S.F. Obada: Influence of the Coupling between Two Qubits in an Open Coherent Cavity: Nonclassical Information via Quasi-Probability Distributions. *Entropy* **2019**, *21*, 1137. [[CrossRef](#)]
57. Mohamed, A.-B.A. Long-time death of nonclassicality of a cavity field interacting with a charge qubit and its own reservoir. *Phys. Lett. A* **2010**, *374*, 4115.
58. Liu, Y.-X.; Wei, L.F.; Nori, F. Preparation of macroscopic quantum superposition states of a cavity field via coupling to a superconducting charge qubit. *Phys. Lett. A* **2005**, *71*, 063820. [[CrossRef](#)]

59. Pashkin, Y.A.; Yamamoto, T.; Astafiev, O.; Nakamura, Y.; Averin, D.V.; Tsai, J.S. Quantum oscillations in two coupled charge qubits. *Nature* **2003**, *421*, 823.
60. Abdalla, M.S.; Khalil, E.M.; Obada, A.-S.F. Obada: Exact treatment of the Jaynes-Cummings model under the action of an external classical field. *Ann. Phys.* **2011**, *326*, 2486. [[CrossRef](#)]
61. Barnett, S.M.; Knight, P.L. Dissipation in a fundamental model of quantum optical resonance. *Phys. Rev. A* **1986**, *33*, 2444. [[CrossRef](#)]
62. Puri, R.R.; Agarwal, G.S. Finite-Q cavity electrodynamics: Dynamical and statistical aspects. *Phys. Rev. A* **1987**, *35*, 3433.
63. Moya-Cessa, H.; Knight, P.L. Series representation of quantum-field quasiprobabilities. *Phys. Rev. A* **1993**, *48*, 2479. [[CrossRef](#)]
64. Hessian, H.A.; Mohamed, A.-B.A. Quasi-Probability Distribution Functions for a Single Trapped Ion Interacting with a Mixed Laser Field. *Laser Phys.* **2008**, *18*, 1217. [[CrossRef](#)]
65. Vidal, G.; Werner, R.F. Computable measure of entanglement. *Phys. Rev. A* **2002**, *65*, 032314. [[CrossRef](#)]